Available online at www.sciencedirect.com
ScienceDirect
Advances in Engineering Software 38 (2007) 102–111
ADVANCES IN ENGINEERING SOFTWARE
www.elsevier.com/locate/advengsoft

Bayesian neural networks for prediction of equilibrium and time-dependent scour depth around bridge piers

S. Mohyeddin Bateni [a], Dong-Sheng Jeng [b,*], Bruce W. Melville [c]

[a] Department of Civil and Environmental Engineering, University of Alberta, Edmonton, AB, Canada T6G 2G7
[b] School of Civil Engineering, The University of Sydney, New South Wales 2006, Australia
[c] Department of Civil and Environmental Engineering, The University of Auckland, Auckland, New Zealand

Received 15 July 2005; accepted 7 August 2006
Available online 9 October 2006

Abstract

The physical process of scour around bridge piers is complicated. Despite various models presented to predict the equilibrium scour depth and its time variation from the characteristics of the current and sediment, scope exists to improve the existing models or to provide alternatives to them. In this paper, a neural network technique within a Bayesian framework, is presented for the prediction of equilibrium scour depth around a bridge pier and the time variation of scour depth. The equilibrium scour depth was modeled as a function of five variables; flow depth and mean velocity, critical flow velocity, median grain diameter and pier diameter. The time variation of scour depth was also modeled in terms of equilibrium scour depth, equilibrium scour time, scour time, mean flow velocity and critical flow velocity. The Bayesian network predicted equilibrium and time-dependent scour depth much better when it was trained with the original (dimensional) scour data, rather than using a non-dimensional form of the data. The selection of water, sediment and time variables used in the models was based on conventional scour depth data analysis. The new models estimate equilibrium and time-dependent scour depth more accurately than the existing expressions. A committee model, developed by averaging the predictions of a number of individual neural network models, increased the reliability and accuracy of the predictions. A sensitivity analysis showed that pier diameter has a greater influence on equilibrium scour depth than the other independent parameters.

Keywords: Bayesian neural network; Scour; Bridge piers; Back-propagation algorithm

1. Introduction

The safe and economical design of bridge piers requires accurate prediction of the maximum scour depth around their foundations. Numerous empirical formulae have been presented to estimate equilibrium scour depth at bridge piers under clear water conditions, including Laursen and Toch [20], Shen [32], Hancu [13], Breusers et al. [2], US DOT [34], Melville [24] and Melville and Chiew [25]. These approaches are summarised in Table 1.

Studies of the temporal development of scour at bridge piers include Chabert and Endeldinger [3], Ettema [8], Franzetti et al. [10], Yanmaz and Altinbilek [35], Johnson and McCuen [16], Kothyari et al. [19], Melville and Chiew [25], Oliveto and Hager [29] and Mia and Nago [26].

All aforementioned approaches have been limited to the range of the empirical formulae and experimental data. For the study reported herein, neural network models were applied to existing experimental data for local scour depth at circular bridge piers under steady, clear-water scour conditions in uniform sediments. The neural network approach has been applied to many branches of science, including aspects of hydraulic and environmental engineering. Some of the earliest applications of neural network models in hydrology and water resources engineering were reported by Daniell [7]. More recent applications include Karunanithi et al. [18], Grubert [12], Minns [27], Coppola

* Corresponding author. Tel.: +61 2 9351 2144; fax: +61 2 9351 3343.
E-mail address: d.jeng@civil.usyd.edu.au (D.-S. Jeng).

0965-9978/$ - see front matter © 2006 Elsevier Ltd. All rights reserved.
doi:10.1016/j.advengsoft.2006.08.004

Table 1
The design methods used for comparison in this study[a]

Author	Equation
Laursen and Toch [20]	$d_{se} = 1.35D^{0.7}Y^{0.3}$
Shen [32]	$d_{se} = 0.00022\left(\frac{UD}{\upsilon}\right)^{0.619}$
Hancu [13]	$\frac{d_{se}}{D} = 2.42\left(2\frac{U}{U_c} - 1\right)\left(\frac{U_c^2}{gD}\right)^{1/3}$
Breusers et al. [2]	$\frac{d_{se}}{D} = f\left(\frac{U}{U_c}\right)[2\tanh(\frac{Y}{D})]$ in which $f\left(\frac{U}{U_c}\right) = 0$, for $\frac{U}{U_c} < 0.5$ and $f\left(\frac{U}{U_c}\right) = \left(2\frac{U}{U_c} - 1\right)$, for $0.5 < \frac{U}{U_c} < 1.0$
US DOT [34]	$\frac{d_{se}}{Y} = K_3\left(\frac{Y}{D}\right)^{-0.65}\left(\frac{U}{\sqrt{gY}}\right)^{0.43}$ in which K_3 is a factor that accounts for the state of bed mobility and for the related presence of dunes on approach bed; it varies from 1.1 to 1.3
Melville [24]	$d_{se} = K_{yD}K_IK_dK_sK_\theta K_G$ where K_{yD}, K_I, K_d, K_s, K_θ and K_G are respectively depth size, flow intensity, sediment size, pier shape, pier alignment and channel geometry coefficients
Melville and Chiew [25]	$d_{se} = K_{yD}K_IK_d$ where K_{yD}, K_I and K_d are respectively flow depth-pier width, flow intensity and sediment size coefficients

[a] D = pier diameter; U = average velocity of approach flow; U_c = critical value of U associated with initiation of motion of particles on bed surface; Y = flow depth; υ = kinematic viscosity of water; g = gravitational acceleration, and d_{se} = equilibrium scour depth.

et al. [6], Nagy et al. [28], Jain and Prasad [15], Sudheer and Jain [33]. Recently, Kambekar and Deo [17] estimated scour depth around a group of piles using neural network models.

2. Neural network model

2.1. Neural network framework

In normal regression methods, the analysis begins with the prior choice of a relationship (usually linear) between the output and input variables. A neural network is capable of realizing a greater variety of non-linear relationships of considerable complexity. The data are presented to the network in the form of input and output parameters, and the optimum non-linear relationship is found by minimizing a penalized likelihood. In fact, the network tests many kinds of relationships in its research for an optimum fit. As in regression analysis, the results then consist of a specification of the function, which in combination with a series of coefficients (called weights), relates the inputs to the outputs. The search for the optimum representation can be computed intensive, but once the process is completed (that is, the network has been trained), the estimation of outputs is very rapid. The neural network can be susceptible to over-fitting. We will use a Bayesian framework [21] to control this problem.

MacKay [21–23] developed a Bayesian framework for neural networks. This framework allows quantitative assessment of the relative probabilities of models of different complexity, and quantitative errors can be applied to the predictions of the models. This work has been applied to the complex problem of predicting scour depth around bridge piers and its time variation in the study reported herein.

Fig. 1 shows the structure of the neural network used in our model. A set of data $(x_1, x_2, \ldots)$ is firstly fed directly into the network through the input layer and, subsequently, the Bayesian neural network produces an expected result (y) in the output layer. The output (y) is determined by the architecture of the network.

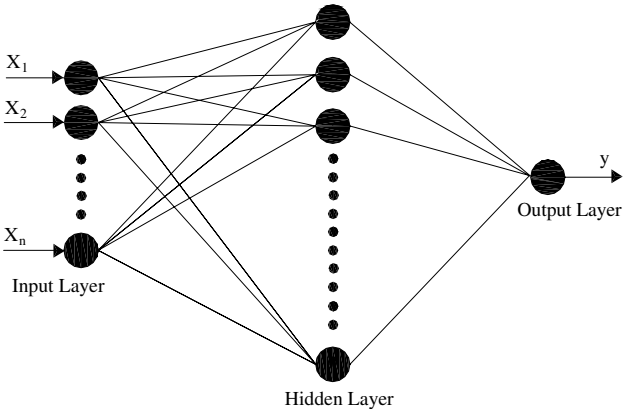

Fig. 1. Neural network model in this study.

To predict the output, i.e., the scour depth, hidden nodes were used between the inputs and the output so that more complex relationships could be expressed. The transfer function relating the inputs to the ith hidden nodes is given by

$$h_i = \tanh\left(\sum_j w_{ij}^{(1)}x_j + \theta_i^{(1)}\right). \quad (1)$$

The relationship between the hidden nodes and the output is linear, that is

$$y = \sum_i w_i^{(2)}h_i + \theta^{(2)}. \quad (2)$$

The coefficient w and biases θ of these equations are determined in such a way as to minimize the energy function, as explained later. Because the hyperbolic function is a non-linear function, a non-linear relationship can be predicted using this model.

2.2. Training of neural network

Both the input and output variables were first normalized within the range 0–1 as follows:

$$x_{\mathrm{N}} = \frac{x - x_{\min}}{x_{\max} - x_{\min}}, \tag{3}$$

where x_{N} is the normalized value of x, $x_{\max}$ is the maximum value and $x_{\min}$ is the minimum value of each variable of the original data. This normalization is not essential to the neural network approach, but allows the network to be trained better.

Using the normalized data, the coefficients (weights) w and bias θ were determined in such a way as to minimize the following energy function [21]:

$$M(w) = \beta E_{\mathrm{D}} + \sum_{c} \alpha_c E_{w(c)}. \tag{4}$$

The minimization was implemented using a variable metric optimizer [30]. The gradient of $M(w)$ was computed using a back-propagation algorithm [31]. The energy function consists of the error function, E_{D} and regularization, E_w. The error function is the sum-squared error as follows:

$$E_{\mathrm{D}}(w) = \frac{1}{2}\sum_{m=1}^{N}[y(x^m, w) - t^m]^2, \tag{5}$$

where $\{x^m, t^m\}$ is the data set, x^m represents the inputs, t^m represents the targets, and m is a label of the pair. The error function E_{D} is smallest when the model fits the data well, that is when $y(x^m; w)$ is close to t^m. The coefficients w and biases θ, shown in Eqs. (1) and (2), make up the parameter vector w. A number of regularizers $E_{w(c)}$ are added to the data error. These regularizers favour functions $y(x; w)$, which are smooth functions of x. The simplest regularization method uses a single regularizer, $E_w = \frac{1}{2}\sum w_i^2$. A slightly more complicated regularization method, known as the automatic relevance determination model [22], is used in this study. Each weight is assigned to a class c, depending on which neurons it connects. For each input, all the weights connecting that input to the hidden nodes are in a single class. The biases of the hidden nodes are in another class, and all the weights from the hidden nodes to the outputs are in a final class. $E_{w(c)}$ is defined as the sum of the squares of the weights in class c [21] as follows:

$$E_{w(c)}(w) = \frac{1}{2}\sum_{i \in c} w_i^2. \tag{6}$$

This additional term favor small values of w and decreases the tendency of a model to over-fit noise in the data set.

The control parameters α_c and β, together with the number of hidden nodes, determine the complexity of the model. The most probable value for the weight vector corresponds to the maximum of the posterior probability, or equivalently to the minimum of the right-hand side in (4). Considering a succession of training sets with increasing number N of patterns in (5), then we see that the first term in (4) grows with N while the second term does not. If α_c and β are fixed, then as N increases, the first term becomes more and more dominant, until eventually the second term becomes insignificantly. More detailed discussion regarding the determination of α_c and β can be found in [1].

These hyper-parameters define the assumed Gaussian noise level $\sigma_v^2 = 1/\beta$ and the assumed weight variances, $\sigma_{w(c)}^2 = 1/\alpha_{(c)}$. The noise level inferred by the model is σ_v. The parameter α has the effect of encouraging the weights to decay. Therefore, a high value of σ_w implies that the particular input parameter explains a relatively large amount of the variation in the output. Thus, σ_w is regarded as a good expression of the significance of each input though not of the sensitivity of the output to that input. The values of the hyper-parameters are inferred from the data using the Bayesian methods given in MacKay [21]. In this method, the hyper-parameters were initialized to values chosen by the operator and the weights were set to small initial values. The objective function $M(w)$ was minimized to a chosen tolerance and the values of the hyper-parameters were then updated using a Bayesian approximation given in MacKay [21]. The $M(w)$ function was minimized again, starting from the final state of the previous optimization, and the hyper-parameters were updated again.

2.3. Selecting parameters

Equilibrium scour depth (d_{se}) around a circular pier in a steady flow over a bed of uniform, cohesionless sediment depends on variables characterizing the fluid, flow, bed sediment, and pier (Fig. 2). The following functional relationship describes equilibrium scour depth in terms of its independent parameters [9]:

$$d_{\mathrm{se}} = f(\rho, \mu, U, Y, g, d_{50}, U_{\mathrm{c}}, D) \tag{7}$$

in which ρ = fluid density, μ = fluid dynamic viscosity and d_{50} = particle mean diameter.

The eight dimensional variables are reducible to a set of five non-dimensional parameters. If the variables ρ, U, and D are chosen as repeating variables, the following relationship describes scour depth normalized with pier diameter:

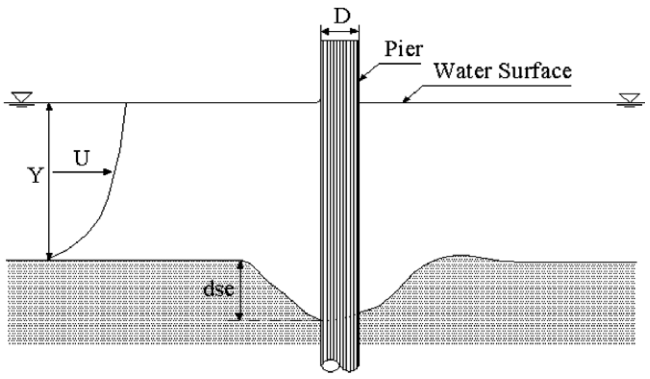

Fig. 2. Flow and local scour around a circular pier.

$$\frac{d_{se}}{D} = \Psi\left(\frac{U}{U_c}, \frac{U}{\sqrt{gY}}, \frac{Y}{D}, \frac{D}{d_{50}}, \frac{\rho UD}{\mu}\right), \tag{8}$$

where $\frac{\rho UD}{\mu}$ is the Reynolds number, $\frac{U}{\sqrt{gY}}$ is the Froude number, and $\frac{D}{d_{50}}$ represents the soil characteristics in terms of grain size (d_{50}). It is noted that (8) is obtained by dimensional analysis with the variables in (7).

Melville and Chiew [25] presented the following formula to predict local scour depth (d_s) at a particular time (t):

$$\frac{d_s}{d_{se}} = \exp\left\{-0.03\left|\frac{U_c}{U}\ln\left(\frac{t}{t_e}\right)\right|^{1.6}\right\}, \tag{9}$$

where t_e is time for equilibrium depth of local scour to develop. According to (9), the relationship between d_s and its dependent parameters can be written

$$d_s = f(d_{se}, U, U_c, t, t_e). \tag{10}$$

Eq. (10) can further be written in the following non-dimensional form:

$$\frac{d_s}{d_{se}} = f\left(\frac{U}{U_c}, \frac{t}{t_e}\right). \tag{11}$$

2.4. Data presentation

The manner in which the data are presented for training is the most important aspect of the neural network method. Often this can be done in more than one way, the best configuration being determined by trial-and-error. It can also be beneficial to examine the input/output patterns or data sets that the network finds difficult to learn. This enables a comparison of the performance of the neural network model for these different combinations of data.

To predict equilibrium scour depth, two combinations of data were considered as inputs. The first combination, which used the original (dimensional) data, involves eight parameters of Eq. (7) as the input pattern and the equilibrium scour depth (d_{se}) as the output pattern. The second combination, which used the dimensionless form of the data, includes five parameters of Eq. (8) and the normalized scour depth (d_{se}/D) as the input and output patterns, respectively.

Also, two combinations of data were used to predict time-dependent scour depth. The first combination involves five parameters of Eq. (10) as the input pattern and the time-dependent scour depth (d_s) as the output pattern and the second combination involves two non-dimensional parameters on the right-hand side of Eq. (11) and the relative scour depth $\left(\frac{d_s}{d_{se}}\right)$ as the input and output patterns, respectively.

2.5. Development of the models

In this study, two types of Bayesian models were developed: (1) single hidden-layer neural network models consisting of only one hidden layer; and (2) multiple hidden-layer neural network models consisting of two and three hidden layers. The task of identifying the number of neurons in the input and output layers is normally simple, as it is dictated by the input and output variables considered to model the physical process.

The performance of all neural network model configurations was based on mean-absolute error (MAE), root-mean-square error (RMSE), and coefficient of determination R^2, of the linear regression line between the predicted values from the neural network model and the desired outputs, as follows:

$$\mathrm{MAE} = \frac{1}{P}\sum_{i=1}^{P}|O_i - t_i|, \tag{12}$$

$$\mathrm{RMSE} = \sqrt{\frac{\sum_{i=1}^{P}(O_i - t_i)^2}{P}}, \tag{13}$$

$$R^2 = 1 - \frac{\sum_{i=1}^{P}(O_i - t_i)^2}{\sum_{i=1}^{P}(O_i - \overline{O}_i)^2}, \tag{14}$$

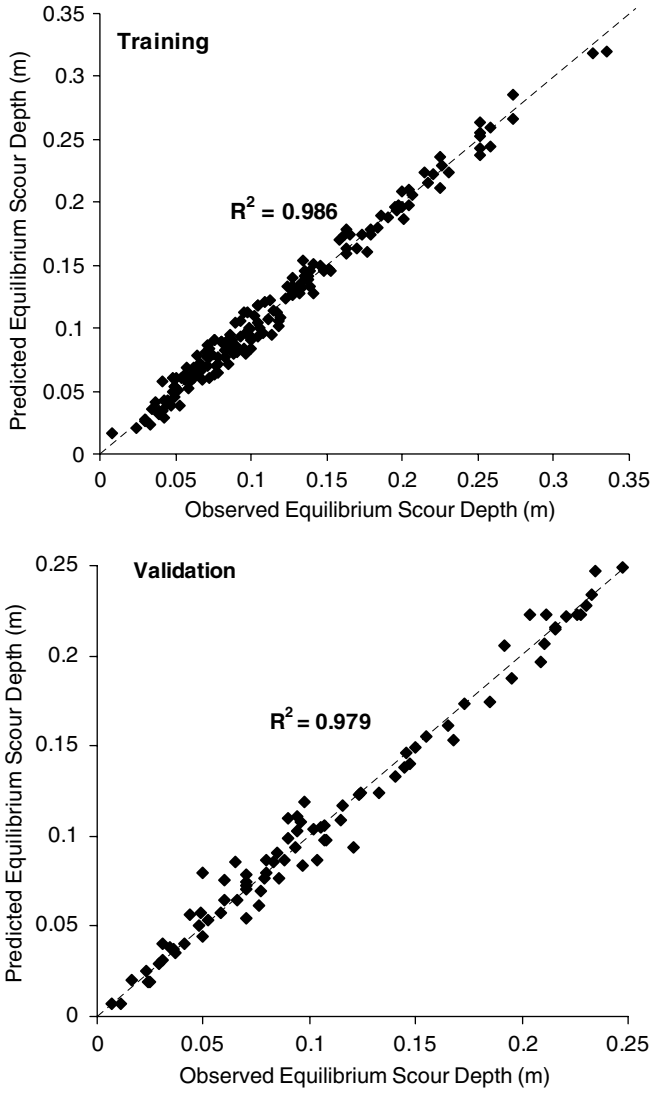

Fig. 3. Plot of observed and predicted (d_{se}) for original data set (Eq. (7)).

where O_i and t_i are target and network output for the ith output, $\overline{O}_i$ is the average of target outputs, and P is the total number of events considered.

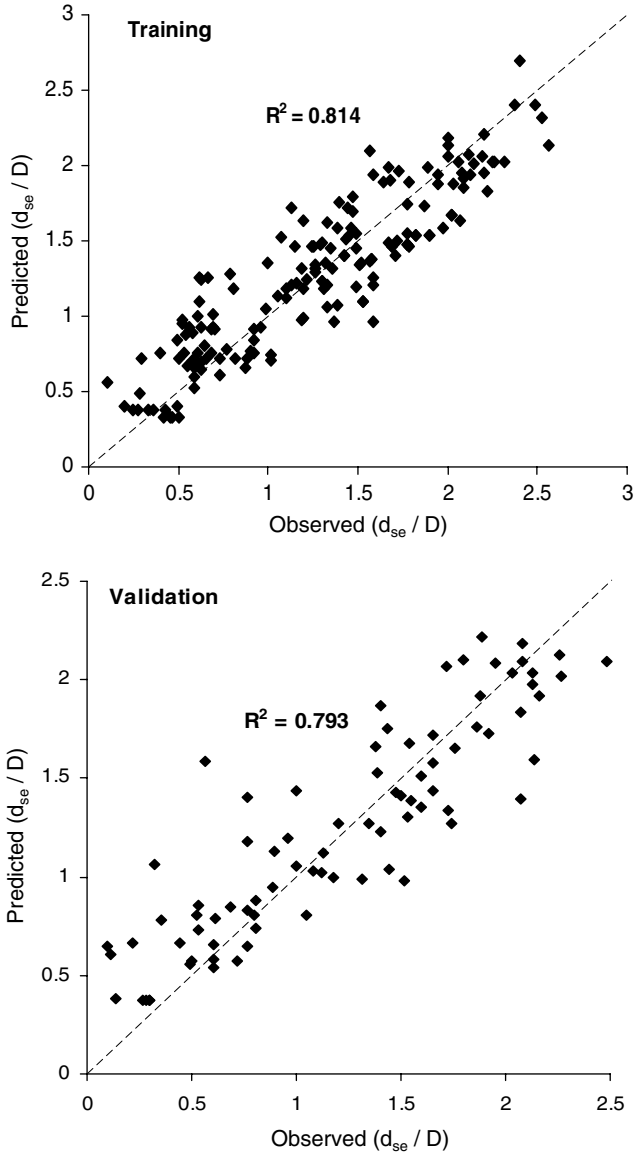

Fig. 4. Plot of observed and predicted $\left(\frac{d_{se}}{D}\right)$ for non-dimensional data set (Eq. (8)).

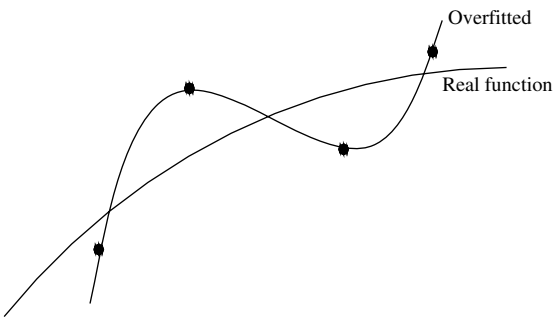

Fig. 5. Over-estimation of function.

Since the appropriate number of hidden layer nodes for the models is not known, a trial-and-error method was used to find the best network configuration. The optimal architecture was determined by varying the number of hidden neurons. The optimal configuration was based upon minimizing the difference among the neural network predicted values and the desired outputs. In general, as the number of hidden layers and the number of neurons within each layer increased, the prediction capabilities of the network also increased significantly.

The training of the neural network models was stopped when either the acceptable level of error was achieved or when the number of iterations exceeded a prescribed maximum of 1000. The neural network model configuration that minimized the MAE and RMSE and optimized the R^2 was selected as the optimum and the whole analysis was repeated several times.

The current study used 20 sets of data to predict equilibrium scour depth from various experimental data [3–5,8,11,13,14,19,24,25,29,35] and unpublished data from the University of Auckland. The whole data set consisting of 263 data points was divided into two parts; a training or

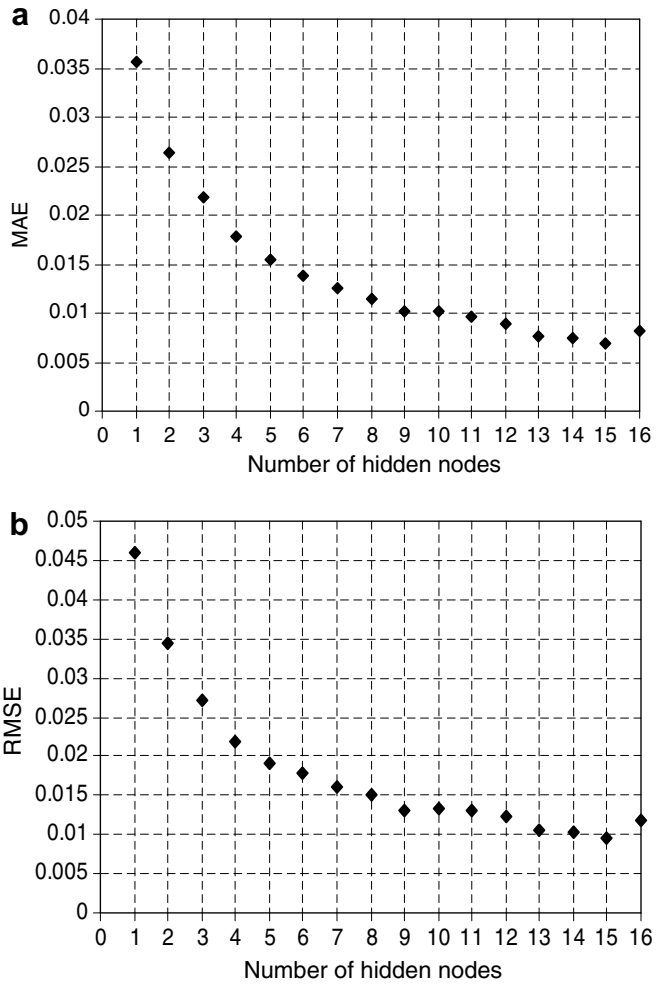

Fig. 6. Error variations of networks for equilibrium scour depth as a function of number of hidden nodes; (a) MAE and (b) RMSE.

calibration set consisting of 180 data points, and a validation or testing set consisting of 83 data points.

The data reported by Melville and Chiew [25], Kothyari et al. [19] and Oliveto and Hager [29] were used to predict scour depth at a particular time t. The whole data set consisting of 1700 data points was divided into two parts; a training set consisting of 1138 data points, and a validation or testing set consisting of 562 data points.

3. Numerical results

The Bayesian models featured small RMSE during training (ranging from 0.0084 m to 0.041 m); however, the value was slightly higher during validation (0.0093–0.046 m). The models showed consistently good correlation throughout the training and testing (>0.8 for all models).

3.1. Comparison of the analyses using the non-dimensional and original data sets as inputs

When networks with different input combinations are compared, the training and testing accuracy does vary significantly. As noted above, two combinations of data were used to predict equilibrium scour depth. Figs. 3 and 4 depict training and validation results, respectively, for the first (dimensional) and second (non-dimensional) combinations of the data. The Bayesian model performed much better when analyzed with the dimensional data set and the parameters of Eq. (7), than when analyzed using the non-dimensional data set and the parameters of Eq. (8).

As the number of hidden nodes increased, the difference between the predicted values and the experimental values decreased. More complex relations can be modeled with a larger number of hidden nodes. However, the function may be then over-fitted, as shown in Fig. 5, because experimental data always contain errors. Figs. 6 and 7 show the change in errors as a function of the number of hidden nodes for the models which yield equilibrium and time-dependent scour depth, respectively. To predict the

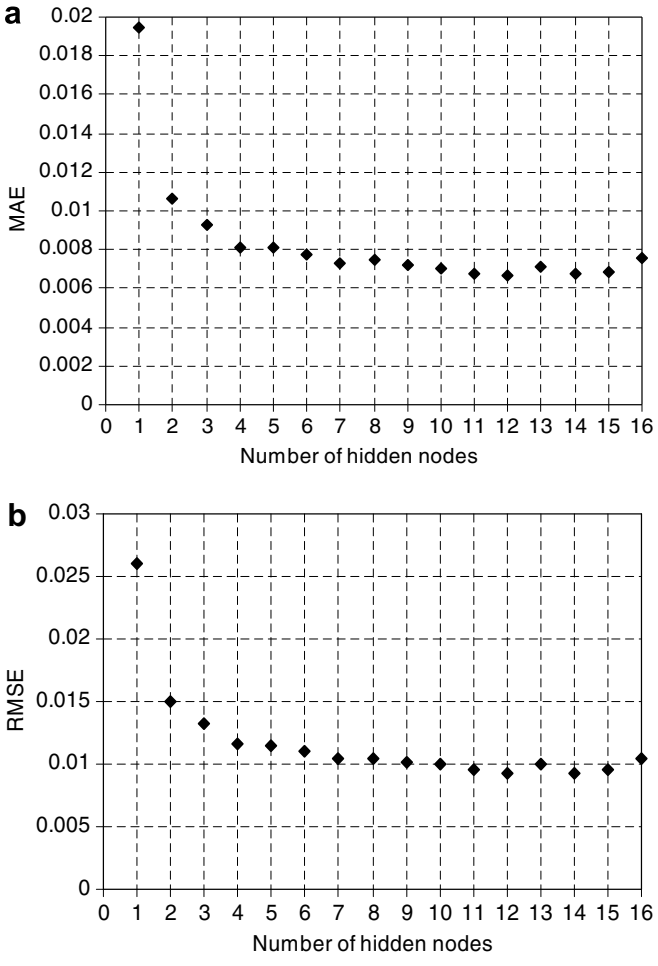

Fig. 7. Error variations of networks for time-dependent scour depth as a function of number of hidden nodes (a) MAE and (b) RMSE.

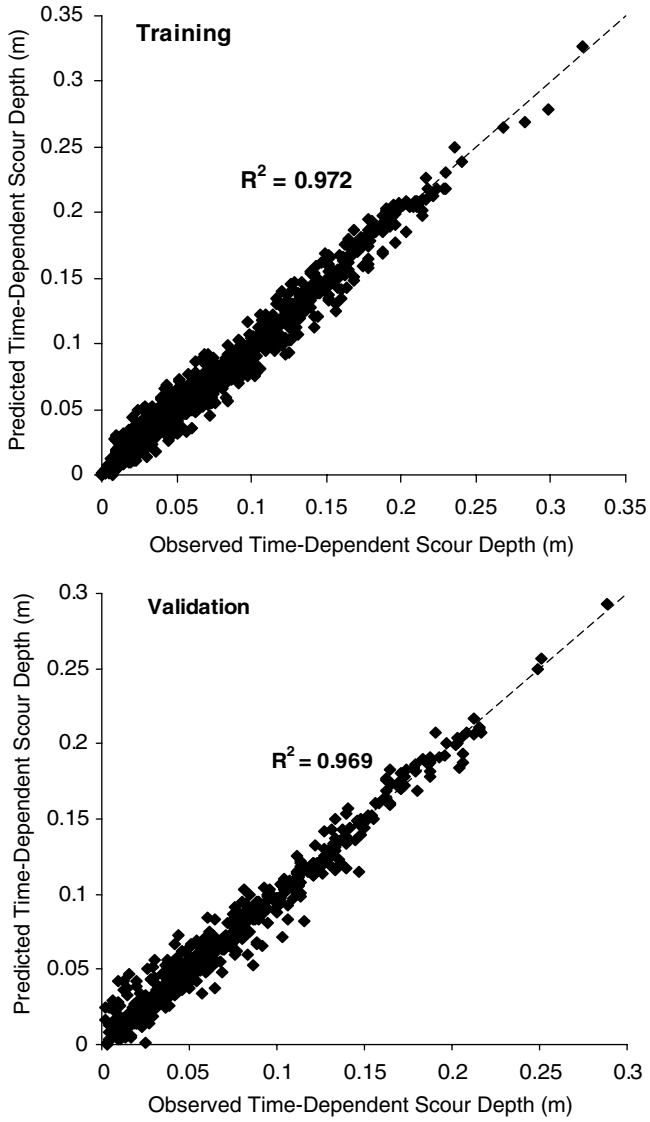

Fig. 8. Plot of observed and predicted time-dependent scour depth (d_s) for original data set (Eq. (9)).

equilibrium scour depth, the network configuration that included two hidden layers and 15 neurons within each hidden layer gave the minimum error (Fig. 6). The network configuration consisting of one hidden layer and 14 neurons within that layer gave the minimum error to predict the temporal variation of scour depth (Fig. 7). These two models were selected as the optimum models.

In a similar manner, two combinations of the data were used to predict time-dependent scour depth. Figs. 8 and 9 show training and validation results for the first and second combinations of the data, respectively. Again, the Bayesian model yielded much better results when analyzed with the first (dimensional) set of data (Eq. (9)), than with the second (non-dimensional) data (Eq. (10)).

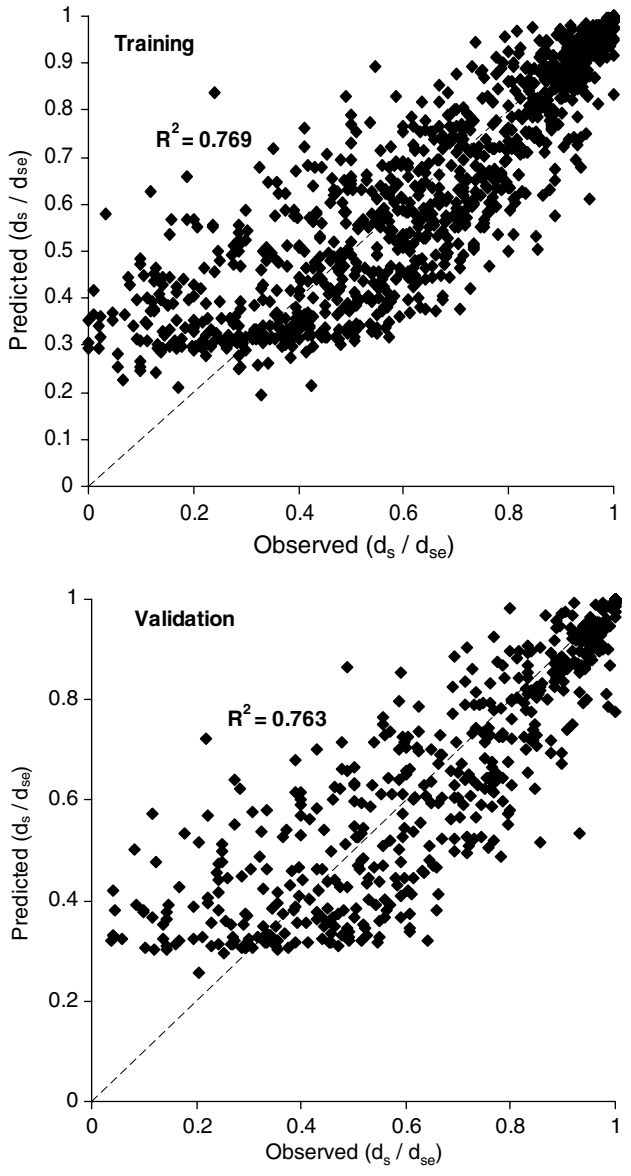

Fig. 9. Plot of observed and predicted relative scour depth $\left(\frac{d_s}{d_{se}}\right)$ for non-dimensional data set (Eq. (10)).

3.2. Committee model

The same data can be modeled in different ways, such as varying the number of hidden nodes, and changing the number of training cycles. The variety of models thus produced can be ranked according to the magnitude of RMSE and the best individual model would then have the minimum RMSE. However, it is possible in principle to reduce the RMSE further by using the average of predictions from a number of models, that is, a committee of models.

In development of a committee model, the individual models were first ranked via their RMSE values. A committee of N models was then formed by combining the best N models, where $N = 1, 2, 3$, etc.

The mean prediction $\bar{y}$ of the committee model is given by

$$\bar{y} = \frac{1}{N}\sum_{i=1}^{N} y_i. \tag{15}$$

Fig. 10 shows the decrease in RMSE for committee models with different N values. The committee models with three (Fig. 10a) and four (Fig. 10b) of the best individual models

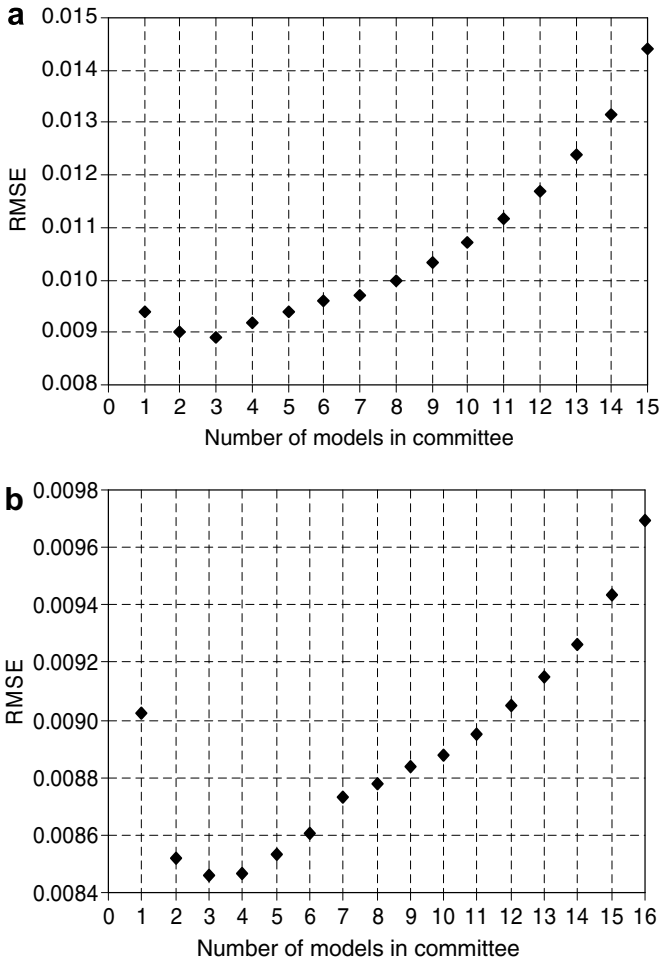

Fig. 10. RMSE variation as a function of number of models in committee. (a) Equilibrium scour depth and (b) time-dependent scour depth.

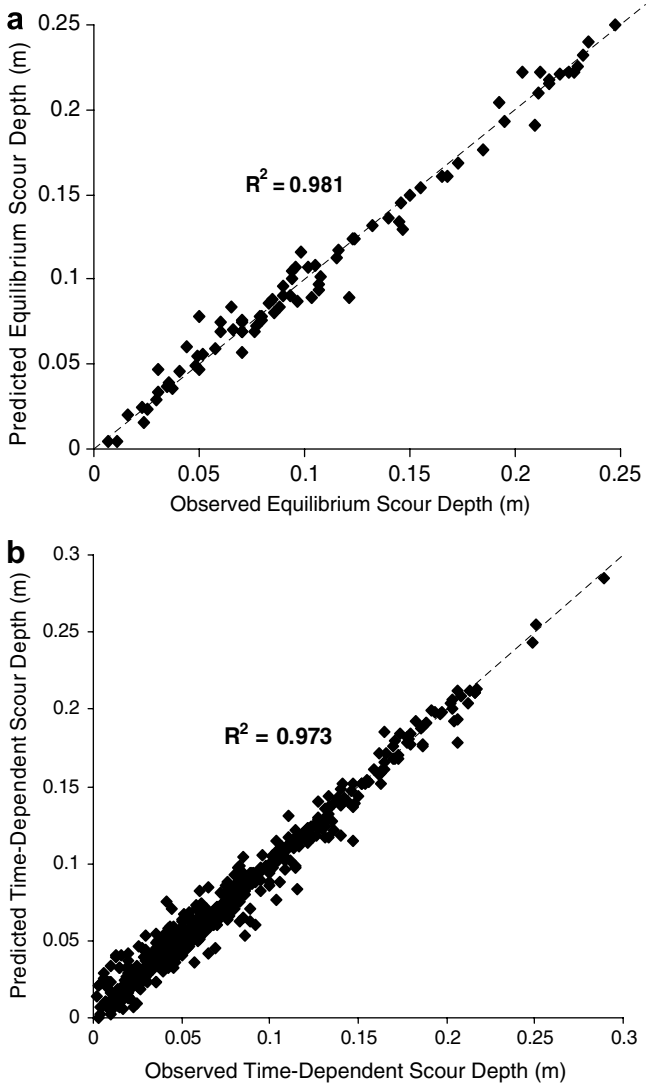

Fig. 11. Comparison between observed and predicted values by committee models. (a) Equilibrium scour depth and (b) time-dependent scour depth.

have a minimum RMSE for equilibrium and time-dependent scour depth, respectively. By using the committee models, the agreement between experimental data and prediction is higher, as shown in Fig. 11.

3.3. Comparison of Bayesian network model with existing scour prediction equations

To evaluate the accuracy of neural network models in predicting equilibrium scour depth, a comparison between the new model and seven of the existing formulae was undertaken using the same 83 observed data set (Table 2). In Table 2 and subsequent tables and figures, ANN stands for artificial neural network. The new model gives improved predictions of scour depth. For the best existing method [34], the RMSE = 0.0463 m, compared to RMSE = 0.0093 m for the new model. Corresponding values of the coefficient of determination are 0.630 and 0.979.

Table 2
Performance indices of various approaches to predict equilibrium scour depth

Different approaches	Errors		Coefficient of determination (R^2)
	MAE (m)	RMSE (m)	
Laursen and Toch [20]	0.0497	0.0727	0.529
Shen [32]	0.0444	0.0640	0.582
Hancu [13]	0.0720	0.1188	0.329
Breusers et al. [2]	0.0613	0.1039	0.122
US DOT [34]	0.0361	0.0463	0.630
Melville [24]	0.0411	0.0589	0.535
Melville and Chiew [25]	0.0393	0.0519	0.607
Present study (ANN)	**0.0066**	**0.0093**	**0.979**

Fig. 12 compares equilibrium scour depth values estimated using the new model and the US DOT [34] method.

Fig. 13 shows time-dependent scour depth values estimated using the new model and the Melville and Chiew [25] method using the same 562 observed data set. As shown, the new model predicts time-dependent scour depth more accurately than Melville and Chiew [24] method.

3.4. Sensitivity analysis

Sensitivity tests were conducted to determine the relative significance of each of the independent parameters (input neurons) on the scour depth (output). Each parameter in Eqs. (7) and (8) was considered in turn in the sensitivity analysis. Table 3 compares the neural network models, with one of the independent parameters removed in each case. The results in Table 3 show that, of the parameters in Eq. (7), pier diameter (D) has the most significant effect on equilibrium scour depth.

Similarly, Table 4 gives sensitivity analysis results for the parameters of Eq. (8). It is apparent that $\left(\frac{y}{D}\right)$ and (Re) have respectively the most and the least effect on normalized

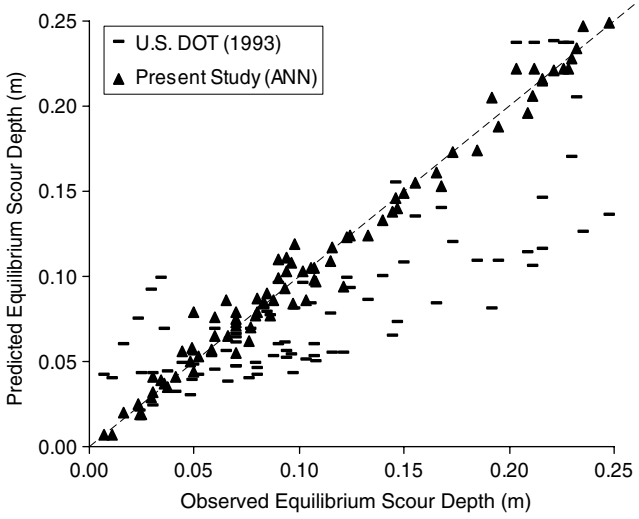

Fig. 12. Comparison between neural network method and US DOT [34] predictions.

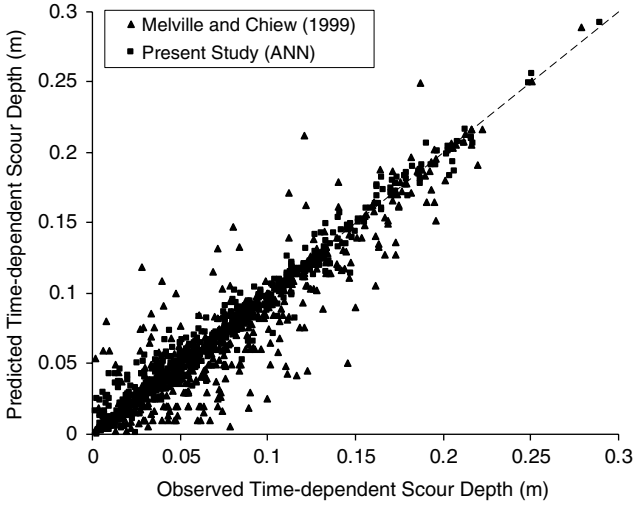

Fig. 13. Comparison between neural network method and Melville and Chiew [25] predictions.

Table 3
Sensitivity analysis results for the parameters in Eq. (7)

Method	MAE	RMSE	Coefficient of determination (R^2)
ANN (Eq. (7))	0.0066	0.0093	0.9790
ANN no U	0.0169	0.0253	0.8491
ANN no U_c	0.0096	0.0133	0.9601
ANN no D	**0.0316**	**0.0435**	**0.5616**
ANN no d_{50}	0.0110	0.0152	0.9474
ANN no Y	0.0100	0.0144	0.9537

Table 4
Sensitivity analysis results for the parameters in Eq. (8)

Method	MAE	RMSE	Coefficient of determination (R^2)
ANN (Eq. (8))	0.2283	0.2991	0.7934
ANN no (U/U_c)	0.2925	0.3727	0.6708
ANN no (Fr)	0.2997	0.4004	0.6397
ANN no (Y/D)	**0.3018**	**0.4112**	**0.5985**
ANN no (D/d_{50})	0.2592	0.3371	0.7332
ANN no (Re)	**0.2112**	**0.2729**	**0.8261**

Table 5
Sensitivity analysis results for the parameters in Eq. (10)

Method	MAE	RMSE	Coefficient of determination (R^2)
ANN (Eq. (10))	0.1293	0.0937	0.7634
ANN no (U/U_c)	0.0957	0.131	0.7569
ANN no (t/t_e)	0.2222	0.2604	0.0407

equilibrium scour depth $\left(\frac{d_{se}}{D}\right)$, considering all of the parameters in Eq. (8). These findings are consistent with existing understanding of the relative importance of the various parameters on scour depth. The effects of the non-dimensional variables on normalized equilibrium scour depth $\left(\frac{d_{se}}{D}\right)$ are seen to be ranked (from higher to lower) in the order $\frac{Y}{D}, Fr, \frac{U}{U_c}, \frac{D}{d_{50}}$ and Re.

Table 5 shows analogous results for time-dependent scour, Eq. (10), with $\left(\frac{t}{t_e}\right)$ being more significant than (U/U_c), as expected.

4. Conclusions

A generalized model for predicting equilibrium and time-dependent scour depth using a Bayesian neural network has been developed. The Bayesian neural network model gives more accurate scour depth predictions than the existing methods. Predictions based on the original (dimensional) scour data were better than those based on dimensionless forms of the data.

The Bayesian network with two hidden layers and 15 hidden nodes within each hidden layer was selected as the optimum network to predict equilibrium scour depth, whereas the network that includes one hidden layer and 14 hidden nodes within that layer was the best model to predict temporal-variation of scour depth.

A committee model was developed to improve the reliability of neural network model predictions. Committee models with three and four of the best individual models for predicting equilibrium and time-dependent scour depth, respectively, performed best.

Sensitivity analysis demonstrated that pier diameter has the most effect on equilibrium scour depth, while $\left(\frac{Y}{D}\right)$ has the most influence on $\left(\frac{d_{se}}{D}\right)$. Also, $\left(\frac{t}{t_e}\right)$ is the most influential parameter on $\left(\frac{d_s}{d_{se}}\right)$.

Acknowledgement

The authors thank Professors Willi H. Hager, Gluseppe Oliveto and Umesh C. Kothyari for providing experimental data.

References

[1] Bishop CM. Neural network for pattern recognition. Oxford: Clarendon Press; 1995.
[2] Breusers HNC, Nicollet G, Shen HW. Local scour around cylindrical piers. J Hydraul Res 1977;15(3):211–52.
[3] Chabert J, Engeldinger P. Etude des affouillements autour des piles des ponts. Laboratoire d' Hydraulique, Chatou, France, 1956 [in French].
[4] Chee RKW. Live-bed scour at bridge piers. Rep. No. 290, School of Engineering, The University of Auckland, New Zealand, 1982.
[5] Chiew YM. Local scour at bridge piers. Rep. No. 355, School of Engineering, The University of Auckland, Auckland, New Zealand, 1984.
[6] Coppola Jr E, Szidarovszky F, Poulton M, Charles E. Artificial neural network approach for predicting transient water levels in a multilayered groundwater system under variable state, pumping, and climate conditions. J Hydrol Eng ASCE 2003;8(6):348–60.
[7] Daniell TM, Neural networks—Application in hydrology and water resources engineering. In: Int Hydro Water Resour Symp, Institute of Engineers, Perth, Australia, 1991. p. 797–802.
[8] Ettema R. Scour at bridge piers. Rep. No. 216, University of Auckland, Auckland, New Zealand, 1980.

[9] Ettema R, Melville BW, Barkdoll B. Scale effect in pier-scour experiments. J Hydraul Eng ASCE 1998;124(6):639–42.
[10] Franzetti S, Larcan E, Mignosa P. Erosione alla base pile circolari di ponti: Verifica sperimentale dell'ipotesi di esistenza una situazione finale di equilibrio. Idrotecnica 1989;16(3):135–41 [Italian].
[11] Graf WH. Load scour around piers. Annu Rep, Laboratoire de Recherches. Hydrauliques, Ecole Polytechnique Federale de Lausanne, Lausanne, Switzerland, 1995. p. B.33.1–8.
[12] Grubert JP. Application of neural networks in stratified flow stability analysis. J Hydraul Eng 1995;121(7):523–32.
[13] Hancu S. Sur le calcul des affouillements locaux dams la zone des piles des ponts. In: Proc 14th IAHR Congress, Paris, France, vol. 3, International Association for Hydraulic Research, Delft, The Netherlands, 1971. p. 299–313.
[14] Jain SC, Fischer EE. Scour around bridge piers at high flow velocities. J Hydraul Eng 1980;106(11):1827–42.
[15] Jain A, Prasad Indurthy SKV. Comparative analysis of event-based rainfall-runoff modeling techniques—deterministic, statistical, and artificial neural networks. J Hydrol Eng 2003;8(2):93–8.
[16] Johnson PA, McCuen RH. A temporal spatial pier scour model. Transp Res Rec 1319, Transportation Research Board, Washington, DC, 1991. p. 143–9.
[17] Kambekar AR, Deo MC. Estimation of group pile scour using neural networks. J Appl Ocean Res 2003;25:225–34.
[18] Karunanithi N, Grenney WJ, Whitly D, Bovee K. Neural networks for river flow production. J Comput Civil Eng 1994;8(2):201–20.
[19] Kothyari UC, Grade RJ, Ranga Raju KG. Temporal variation of scour around circular bridge piers. J Hydraul Eng ASCE 1992;118(8):1091–106.
[20] Laursen EM, Toch A. Scour around bridge piers and abutments. Bulletin No. 4, Iowa Highway Research Board, Ames, Iowa, 1956.
[21] MacKay DJC. Bayes Interpolat Neural Comput 1992;4(3):415–47.
[22] MacKay DJC. A practical Bayesian framework for backpropagation networks. Neural Comput 1992;4(3):448–72.
[23] MacKay DJC. Mathematical modeling of weld phenomena 3. In: Cerjack H, editor. London: The Institute of Materials; 1997, p. 359–89.
[24] Melville BW. Pier and abutment scour: integrated approach. J Hydraul Eng ASCE 1997;123(2):125–36.
[25] Melville BW, Chiew YM. Time scale for local scour depth at bridge piers. J Hydraul Eng 1999;125(1):59–65.
[26] Mia MF, Nago H. Design methods of time-dependent local scour at circular bridge piers. J Hydraul Eng 2003;129(6):420–7.
[27] Minns AW. Artificial neural networks as subsymbolic process descriptors. Rotterdam, The Netherlands: Balkema; 1998.
[28] Nagy HM, Watanabe K, Hirano M. Prediction of sediment load concentration in river using artificial neural network model. J Hydraul Eng ASCE 2002;128(6):588–95.
[29] Oliveto G, Hager WH. Temporal evolution of clear-water pier and abutment scour. J Hydraul Eng 2002;128(9):811–20.
[30] Press WH, Teukolsky SA, Vetterling WT, Flannery BP. Numerical recipes in C. 2nd ed. Cambridge University Press; 1999, p. 418.
[31] Rumelhart DE, Hinton G, Williams R. Learning internal representations by error propagation. Parallel distributed processing: exploration in the microstructure of cognition. In: Rumelhart D, McClelland J, editors. vol. 1, MIT Press, Cambridge, MA, 1986. p. 318–62.
[32] Shen HW. Scour near piers. River Mechanics, vol. II, Ft. Collins, Colo, 1971 [Chapter 23].
[33] Sudheer KP, Jain SK. Radial basis function neural network for modeling rating curves. J Hydrol Eng 2003;8(3):161–4.
[34] US DOT. Evaluating scour at bridges. Hydraul Eng Circular No. 18, FHWA-IP-90-017, Fed Hwy Admin, US Dept of Transp, McLean, VA, 2003.
[35] Yanmaz AM, Altinbilek HD. Study of time-dependent local scour bridge piers. J Hydraul Eng 1991;117(10):1247–68.